FGF21 and its underlying adipose tissue-liver axis inform cardiometabolic burden and improvement in obesity after metabolic surgery

Marie Patt,[a,o] Isabel Karkossa,[b,o] Laura Krieg,[b] Lucas Massier,[a,c] Kassem Makki,[d] Shirin Tabei,[e,f] Thomas Karlas,[g] Arne Dietrich,[h] Martin Gericke,[i] Michael Stumvoll,[a,j] Matthias Blüher,[a,j] Martin von Bergen,[b,k,l] Kristin Schubert,[b] Peter Kovacs,[a,m] and Rima M. Chakaroun[a,n,*]

[a]University of Leipzig Medical Centre, Medical Department III–Endocrinology, Nephrology, Rheumatology, Leipzig, Germany
[b]Department of Molecular Systems Biology, Helmholtz-Centre for Environmental Research - UFZ, Leipzig, Germany
[c]Department of Medicine (H7), Karolinska Institutet, Stockholm, Sweden
[d]INSERM U1060, INRAE UMR1397, Université de Lyon, France
[e]Institute of Endocrinology and Diabetes, University of Lübeck, Lübeck, Germany
[f]Centre of Brain, Behaviour, and Metabolism (CBBM), University of Lübeck, Lübeck, Germany
[g]Division of Gastroenterology, Medical Department II, University of Leipzig Medical Centre, Leipzig, Germany
[h]Department of Visceral, Transplant, Thoracic and Vascular Surgery, University of Leipzig Medical Centre, Leipzig, Germany
[i]Leipzig University, Institute of Anatomy, Leipzig, Germany
[j]Helmholtz Institute for Metabolic Obesity and Vascular Research (HI-MAG), Helmholtz Zentrum München, University of Leipzig and University Hospital Leipzig, Leipzig, Germany
[k]Institute of Biochemistry, Leipzig University, Leipzig, Germany
[l]German Centre for Integrative Biodiversity Research (iDiv) Halle-Jena-Leipzig, Leipzig, Germany
[m]Deutsches Zentrum für Diabetesforschung e.V., 85764, Neuherberg, Germany
[n]Wallenberg Laboratory, Department of Molecular and Clinical Medicine and Sahlgrenska Centre for Cardiovascular and Metabolic Research, University of Gothenburg, Gothenburg, Sweden

eBioMedicine
2024;110: 105458
Published Online xxx
https://doi.org/10.1016/j.ebiom.2024.105458

Summary

Background This research investigates the determinants of circulating FGF21 levels in a cohort reflecting metabolic disease progression, examining the associations of circulating FGF21 with morphology and function of adipose tissue (AT), and with metabolic adjustments following metabolic surgery.

Methods We measured serum FGF21 in 678 individuals cross-sectionally and in 189 undergoing metabolic surgery longitudinally. Relationships between FGF21 levels, AT histology, transcriptomes and proteomes, cardiometabolic risk factors, and post-surgery metabolic adjustments were assessed using univariate and multivariate analyses, causal mediation analysis, and network integration of AT transcriptomes and proteomes.

Findings FGF21 levels were linked to central adiposity, subclinical inflammation, insulin resistance, and cardiometabolic risk, and were driven by circulating leptin and liver enzymes. Higher FGF21 were linked with AT dysfunction reflected in fibro-inflammatory and lipid dysmetabolism pathways. Specifically, visceral AT inflammation was tied to both FGF21 elevation and liver dysfunction. Post-surgery, FGF21 peaked transitorily at three months. Mediation analysis highlighted an underlying increased AT catabolic state with elevated free fatty acids (FFA), contributing to higher liver stress and FGF21 levels (total effect of free fatty acids on FGF21 levels: 0.38, $p < 0.01$; proportion mediation via liver 32%, $p < 0.01$). In line with this, histological AT fibrosis linked with less pronounced FGF21 responses and reduced fat loss post-surgery (FFA and visceral AT fibrosis: rho = –0.31, $p = 0.030$; FFA and fat-mass loss: rho = 0.17, $p = 0.020$).

Interpretation FGF21 reflects the liver's disproportionate metabolic stress response in both central adiposity and after metabolic surgery, with its dynamics reflecting an AT-liver crosstalk.

Funding This work was supported by the Deutsche Forschungsgemeinschaft (DFG, German Research Foundation) through CRC 1052, project number 209933838, CRC1382 and a Walther-Benjamin Fellowship and by a junior research grant by the Medical Faculty, University of Leipzig, and by the Federal Ministry of Education and Research (BMBF), Germany, FKZ: 01EO1501. Part of this work was supported by the European Union's Seventh Framework

*Corresponding author. University of Leipzig Medical Centre, Medical Department III–Endocrinology, Nephrology, Rheumatology, Leipzig, Germany.
E-mail address: rima.chakaroun@wlab.gu.se (R.M. Chakaroun).
[o]These authors contributed equally.

Program for research, technological development and demonstration under grant agreement HEALTH-F4-2012-305312 and by the CRC1382 and the Novo Nordisk Foundation and by the Deutsche Forschungsgemeinschaft (DFG, German Research foundation) project number 530364326.

Keywords: Metabolic surgery; Insulin resistance; Obesity; Metabolic disease; Adipose tissue; FGF21; Inter-organ crosstalk

Research in context

Evidence before this study

FGF21, primarily secreted by the liver, plays a crucial role in reducing insulin resistance and hepatic steatosis, but is paradoxically increased in obesity and type 2 diabetes. Notably, FGF21 levels have been suggested to play a role in improving insulin sensitivity after metabolic surgery, despite varied reported responses in FGF21 levels post-Roux-en-Y gastric bypass and other weight loss strategies. This study explores how metabolic characteristics and adipose tissue (AT) architecture relate to circulating FGF21 levels, how these levels change following metabolic surgery, and how they relate to the metabolic outcomes of the surgical intervention.

Added value of this study

FGF21 reflects cardiometabolic burden, and leptin is its' top predictor. Post-surgery, FGF21 maintained its positive relationship with cardiometabolic burden but peaked at three months and decreased at 12 months below baseline levels. Short-term FGF21-increase were indicative of a catabolic liver response and associated with greater weight and fat loss at one year. This short-term increase was dependent on AT-characteristics modulating fatty acid availability including AT fibrosis, suggesting that FGF21 levels may be influenced by hepatic FFA influx from AT with maintained lipolysis both in insulin resistance and following metabolic surgery, two sides of the "metabolic stress" coin.

Implications of all the available evidence

This study highlights the role of FGF21 in indicating AT-liver crosstalk and suggests that short-term dynamics of FGF21 can serve as a surrogate for AT-health and metabolic surgery success. It questions FGF21's direct role in glycaemic improvements, potentially guiding future research, and clinical practice.

Introduction

Obesity, a chronic and relapsing disease characterized by increased adiposity[1] and adipose tissue dysfunction,[2] is the leading cause of cardiometabolic morbidity and mortality worldwide.[3] Notably, even modest weight loss can lead to significant metabolic and cardiovascular improvements.[4] Metabolic surgery, in particular, yields substantial, long-term weight loss and significantly improves remission rates of metabolic syndrome (MetS) and type 2 diabetes (T2D).[5] Changes in cytokine and hormonal signatures both in obesity and following metabolic surgery highlight the need to investigate putative metabolic regulators.

Fibroblast growth factor 21 (FGF21) is one such regulator, predominantly expressed in the liver and to lesser extents in the brain and pancreas under basal conditions. It is mainly secreted by the liver under stress stimuli, like enhanced lipoprotein catabolism and lipolysis, in prolonged fasting and mitochondrial stress.[6,7] FGF21 was first identified in 2005 as an insulin sensitizer, promoting glucose uptake in adipocytes via GLUT-1 upregulation in cell culture. Subsequent research has clarified potential *in vivo* glucoregulatory actions stemming from the inhibition of hepatic glucose output, enhanced peripheral glucose disposal, and insulin sensitivity.[8] These metabolic effects seem to be, at least partly, mediated by the FGF receptor 1 (FGFR1) in white adipose tissue (WAT), governing whole-body energy homeostasis and suggesting relevant crosstalk between the liver and adipose tissue.[9,10] Clinically, FGF21 analogues reduced hepatic steatosis[11] and improved fasting glucose and whole-body insulin sensitivity in individuals with obesity and T2D,[12] but their impact on glycaemic control has been inconsistent across studies.[13]

Counterintuitively, FGF21 levels are elevated in obesity, T2D, and MetS,[14,15] and divergent evidence suggests a decrease after weight loss. Although this trend varies depending on the weight loss method and the timing of measurement: While a small study showed no significant FGF21 changes one-year post-surgery, Roux-en-Y gastric bypass (RYGB) reportedly increases FGF21 levels, in contrast to dieting, which tends to decrease them.[7,16–18] These observations contrast with reports of FGF21 elevations after several days of fasting.[7] Additionally, the observed positive correlation between changes in the Homeostasis Model Assessment of insulin resistance (HOMA-IR) and FGF21 levels following weight loss, albeit not always reproducible due to the limited sample sizes, has led researchers to propose a potential role for FGF21 in the resolution of T2D in metabolic surgery.[16,17,19] Importantly, it is unclear whether WAT characteristics are relevant to FGF21 levels both under homeostatic metabolic conditions and following metabolic surgery.

In this study, we hypothesize that variations in circulating FGF21 levels link to the severity of metabolic diseases such as type 2 diabetes, hypertension, and dyslipidaemia, and to characteristics of "metabolically sick" AT including histological features (such as macrophage infiltration, adipocyte-size, and -counts and fibrotic status), transcriptomes and proteomes. We further propose that metabolic surgery will alter FGF21 levels, correlating with changes of important health markers such as obesity status, T2D remission, and insulin resistance. Additionally, we expect baseline and post-surgery FGF21 dynamics to reflect interactions between baseline AT status and the liver. To explore these hypotheses, the following objectives were defined: In a cross-sectional cohort of 678 deeply phenotyped individuals, we aim to (I) identify the top predictors of circulating FGF21 and (II) determine transcriptomic, proteomic and histological characteristics of visAT and scAT that associate with circulating FGF21 levels. In the longitudinal subgroup of 189 individuals who underwent metabolic surgery, we aim to (III) quantify the effects of metabolic surgery on anthropometric and cardiometabolic characteristics and FGF21, (IV) identify whether the FGF21 dynamic post-surgery relates to improvement of insulin resistance and cardiometabolic risk and (V) elucidate predictive value of FGF21 at baseline and dynamic for improvement of insulin resistance, T2D remission, weight-, and fat loss.

Methods

Study participants

678 participants were recruited to the University Hospital of Leipzig, Germany (Table 1). These individuals had various degrees of metabolic impairment (normal weight without the metabolic syndrome (nonMS), obesity, T2D or both T2D and obesity). Of these, 189 individuals in a longitudinal subgroup underwent metabolic surgery (RYGB, n = 168; VSG, n = 21) and were followed up at three and 12-months post-surgery (Table 2). Exclusion criteria were inflammatory disorders, chronic renal disease, coronary artery disease, and pregnancy/breastfeeding. Baseline data were collected two months before surgery. T2D resolution after 12 months was defined as HbA1c < 5.7%, fasting glucose <5.6 mmol/l, and no antidiabetic medication.

Obesity was defined as a BMI ≥ 30 kg/m^2 (ICD-10-GM 2021 criteria). T2D was diagnosed using the American Diabetes Association (ADA) 2019 criteria[20] and assessed dichotomously, while other forms were excluded based on clinical presentation, c-peptide, and auto-antibodies detection. Nutritional intake was evaluated using Food Frequency Questionnaires (FFQs) based on the European Prospective Investigation of Cancer (EPIC)-Norfolk-FFQ.[21]

In all participants, including individuals followed-up after metabolic surgery, phenotyping encompassed clinical and anthropometric phenotyping (physical exams, blood pressure, ECG body weight, height, BMI, waist-to-hip ratio [WHR], body impedance analysis using BC-418 MA, Tanita, Japan), and blood sampling by venepuncture for biochemical analyses including metabolic laboratory measurements of glucose and lipid metabolism (fasting glucose, insulin, c-peptide, triglycerides, total, HDL- and LDL-cholesterol, free fatty acids), liver (ALT, AST, GGT), kidney function (eGFR), inflammatory and haematological parameters (complete blood count, CRP) and FGF21 measurements. Participants' sex was self-reported. Leptin and IL-6 were measured in the cross-sectional setting in the 678 individuals. Adipose tissue samples were taken from a subgroup of individuals undergoing metabolic surgery (Table S1) and were subjected to histological, transcriptomic and proteomics analyses as detailed below. Insulin resistance was indirectly measured using HOMA-IR (calculated as (fasting serum glucose (mmol/l) x fasting serum insulin (mlU/l))/22,5).[22] After metabolic surgery the participants were grouped by their responsiveness in terms of weight loss. Percentage Total Weight Loss (%TWL) was calculated as ((initial weight–weight at 12 months)/initial weight) * 100. Weight loss response was categorized based on %TWL, with <20% indicating a poor response and ≥20% a good response.[23]

Ethics

The study protocols were approved by the University of Leipzig's ethics committee (applications 017-12-23012012 and 047-13-28012013[24,25]), with all participants providing written informed consent. The study complied with the ethical approvals.

Biochemical analyses including FGF21 measurements

Blood samples, taken after overnight fasting, were centrifuged immediately and stored at –80 °C for subsequent analysis. Kidney and liver functions, along with blood metabolic markers, were evaluated using standard clinical laboratory methods. Levels of interleukin 6 (IL6) and FGF21 were measured using ELISA kits (IL-6 and FGF21 catalogue numbers: RD194015200R and RD1981108200R, respectively, Biovendor, Czech Republic), following the manufacturers' instructions. Sample absorbance was read in duplicates at 450 nm and referenced at 630 nm using a Tecan sunrise instrument (TECAN GmbH, Germany). The intra-assay and inter-assay coefficient of variation (CV) were 2.7% and 14.1%, respectively.

AT histology

During metabolic surgery, abdominal subcutaneous and visceral WAT (scAT and visAT) biopsies were collected from 59 individuals (Table S1). Samples were either immediately frozen in liquid nitrogen and stored at –80 °C or fixed in 4% paraformaldehyde at 4 °C for

	nonMS		T2D		Obesity		Obesity + T2D		p	n
n	101		96		247		234			678
Sex (f/m)	26/75	bcd	63/33	acd	99/148	ab	115/119	ab	$\mathbf{6.5 \times 10^{-8}}$	678
Age (years)	51 [36; 64]	bcd	67 [62; 71]	acd	45 [34; 53]	abd	60 [51; 65]	abc	$\mathbf{4.9 \times 10^{-47}}$	678
FGF21 (pg/ml)	87.9 [48.3; 178.1]	bcd	222.5 [148.9; 421.0]	ac	175.8 [101.7; 298.9]	abd	289.3 [172.3; 488.2]	ac	$\mathbf{4.2 \times 10^{-25}}$	687
BMI (kg/m^2)	22.6 ± 2.0	bcd	27.8 ± 1.6	acd	45.5 ± 7.4	abd	41.5 ± 9.5	abc	$\mathbf{3.5 \times 10^{-96}}$	678
WHR	0.8 ± 0.1	bcd	1.0 ± 0.1	acd	0.9 ± 0.1	abd	1.0 ± 0.1	abc	$\mathbf{6.2 \times 10^{-39}}$	630
TFM (kg)	16.3 ± 5.8	bcd	24.9 ± 5.7	acd	62.9 ± 16.9	abd	52.8 ± 21.2	abc	$\mathbf{4.0 \times 10^{-92}}$	672
Visceral fat rating	5.5 ± 3.1	bcd	13.0 ± 2.9	acd	18.6 ± 7.1	ab	18.8 ± 7.0	ab	$\mathbf{6.9 \times 10^{-64}}$	632
Systolic BP (mmHg)	118.7 ± 14.6	bcd	136.9 ± 13.5	ac	127.8 ± 14.2	abd	132.7 ± 15.1	ac	$\mathbf{3.7 \times 10^{-18}}$	635
Diastolic BP (mmHg)	67.4 ± 8.9	bcd	73.2 ± 10.4	a	74.5 ± 11.2	a	74.0 ± 11.5	a	$\mathbf{1.0 \times 10^{-7}}$	635
FPG (mmol/l)	4.9 [4.6; 5.3]	bd	7.1 [6.1; 8.6]	ac	5.3 [4.9; 5.7]	abd	7.6 [6.2; 9.0]	ac	$\mathbf{1.3 \times 10^{-71}}$	674
HbA1c (%)	5.3 [5.2; 5.5]	bd	6.5 [6.1; 7.1]	ac	5.6 [5.4; 5.8]	abd	6.7 [6.1; 7.3]	ac	$\mathbf{1.0 \times 10^{-85}}$	676
FPI (mIU/l)	4.8 [3.9; 6.5]	bcd	10.4 [7.6; 16.3]	acd	16.6 [11.3; 21.9]	ab	18.6 [11.5; 32.7]	ab	$\mathbf{2.1 \times 10^{-50}}$	610
HOMA-IR	1.0 [0.8; 1.5]	bcd	3.4 [2.2; 5.9]	ad	3.9 [1.6; 5.4]	ad	6.9 [3.5; 13.6]	abc	$\mathbf{4.9 \times 10^{-55}}$	610
Total chol. (mmol/l)	5.3 ± 1.1		5.0 ± 1.0		5.1 ± 1.1		5.1 ± 1.1		0.183	678
HDL-chol.(mmol/l)	1.9 [1.6; 2.2]	bcd	1.3 [1.1; 1.6]	a	1.3 [1.1; 1.5]	a	1.2 [1.0; 1.4]	a	$\mathbf{5.5 \times 10^{-30}}$	678
LDL-chol. (mmol/l)	3.2 ± 1.0		3.0 ± 0.8		3.3 ± 0.9		3.1 ± 0.9		0.125	678
Triglycerides (mmol/l)	0.9 [0.6; 1.3]	bcd	1.5 [1.2; 1.3]	a	1.5 [1.1; 1.9]	ad	1.7 [1.3; 2.3]	ac	$\mathbf{2.4 \times 10^{-27}}$	678
eGFR CKD-EPI (ml/min per 1.73 m^2)	85.6 [77.6; 94.2]	c	83.8 [74.6; 95.4]	c	95.3 [82; 106]	abd	86.3 [71.5; 100.5]	c	$\mathbf{1.9 \times 10^{-7}}$	677
Microalbuminuria (mg/l)	3.0 [3.0; 8.0]	bd	8.5 [3.5; 24.0]	ac	4.3 [3.0; 11.7]	bd	9.5 [3.0; 30.5]	ac	$\mathbf{9.7 \times 10^{-9}}$	617
AST (U/l)	24.0 [20.4; 26.9]	bcd	26.9 [22.8; 32.2]	ad	25.7 [22.2; 32.3]	a	30.5 [24.0; 38.6]	ab	$\mathbf{2.5 \times 10^{-9}}$	677
ALT (U/l)	17.4 [14.4; 22.2]	bcd	26.9 [20.7; 35.2]	a	26.9 [20.4; 38.9]	a	31.2 [22.6; 45.5]	a	$\mathbf{2.3 \times 10^{-23}}$	677
CRP (mg/l)	0.7 [0.3; 1.5]	bcd	2.2 [1.3; 4.6]	acd	7.3 [3.5; 13.3]	ab	5.4 [2.4; 11.9]	ab	$\mathbf{1.1 \times 10^{-44}}$	677

Abbreviations: nonMS: no metabolic syndrome, T2D: type 2 diabetes. BMI: body mass index, WHR: waist-to-hip ratio, TFM: total fat mass, BP: blood pressure, FPG: fasting plasma glucose, HbA1c: glycated haemoglobin, FPI: fasting plasma insulin, HOMA-IR: homeostatic model assessment of insulin resistance, HDL: high density lipoprotein, LDL: low density lipoprotein, eGFR CKD-EPI: estimated glomerular filtration rate, AST: aspartate aminotransferase, ALT: alanine aminotransferase, CRP: c-reactive protein, IL6: interleukin 6. All normally distributed values as mean ± standard deviation, others as median [25. percentile; 75. percentile]. Differences between groups were analysed by Kruskal–Wallis ANOVA and between two individual groups with Mann–Whitney U test for independent groups. Differences in sex distribution was analysed by x2 analysis. The Letter code indicates: (a) $p < 0.05$ vs nonMS, (b) $p < 0.05$ vs T2D, (c) $p < 0.05$ vs obesity, (d) $p < 0.05$ vs obesity + T2D.

Table 1: **Cohort characteristics grouped into nonMS, obesity, T2D, obesity + T2D.**

48 h, then embedded in paraffin and sectioned into 6 µm slices. Adipocyte size and counts, macrophages, and crown-like structures were quantified as previously detailed.[24] ScAT fibrosis was assessed by staining for type I and III collagen using picrosirius-red, with the ratio of collagen to total tissue area indicating fibrosis levels.[26] Fibrosis was classified as perilobular (PLF) and pericellular (PCF), each scored from 0 (none or very limited) to 2 (severe). A combined semiquantitative fibrosis score (FAT-score) was assigned to each sample in a blinded fashion, ranging from 0 (no fibrosis) to 3 (severe PLF and PCF).[24]

AT transcriptomics and proteomics

We examined transcriptomics and proteomics data[24] from scAT and visAT samples of the longitudinal subgroup (Table S1). The log2-transformed, normalized data from these tissues were screened for outliers as previously described.[24] Data free of outliers (excluding two scAT and visAT transcriptome samples and three scAT proteome samples) were used to assess Spearman's rank correlations with baseline FGF21 levels, focusing on the top 25 positively and negatively significantly correlating transcripts or proteins (with ENSG IDs) (Tables S2–S5, 10.5281/zenodo.13730671).

Significant protein-transcript overlaps were identified using Uniprot-to-ENSG ID mappings via DAVID.[27] Weighted Gene Correlation Network Analyses (WGCNAs)[24] were performed for transcriptomes and proteomes, applying the default parameters with the specified exceptions (scAT transcriptome: maxBlockSize = 25,000, soft-threshold = 7, module size = 500–5000; visAT transcriptome: soft-threshold = 5; scAT proteome: maxBlockSize = 5000, soft-threshold = 7, module size = 50–200). With these analyses, signed networks were formed based on the co-abundance of the analytes (here: transcripts or proteins). These networks were cut into modules of co-abundant analytes. Thus, the analytes within one module share the same or at least a very similar abundance profile over the samples investigated, resulting in the potential that they may be involved in similar biological

	RYGB				VSG			
	Baseline	n	Three months	12 months	Baseline	n	Three months	12 months
n	168				21			
Sex (f/m)	103/65				09/12			
Age (years)	48.0 ± 11.1				44.9 ± 10.8			
FGF21 (pg/ml)	270.3 [148.0; 440.4]	168	465.5 [223.3; 812.0]	175.1 [94.6; 312.8]	271.1 [130.0; 364.1]	21	461.2 [299.0; 742.7]	164.4 [80.0; 323.0]
BMI (kg/m2)	48.7 ± 6.0	167	40.4 ± 6.0	34.6 ± 5.8	56.9 ± 7.5	21	46.5 ± 7.0	40.0 ± 7.5
TFM (kg)	67.7 [57.2; 78.0]	163	50.5 [39.7; 58.5]	36.5 [26.5; 45.1]	76.6 [63.1; 100.7]	20	61.6 [51.4; 71.2]	39.7 [29.7; 51.4]
Systolic BP (mmHg)	131.8 ± 15.1	131	119.0 ± 14.1	119.2 ± 15.1	130.2 ± 12.0	20	114.2 ± 16.5	117.2 ± 10.1
Diastolic BP (mmHg)	76.1 ± 12.6	131	68.3 ± 10.9	69.1 ± 10.9	68.7 ± 10.4	20	62.6 ± 8.7	65.7 ± 8.3
FPG (mmol/l)	5.8 [5.2; 6.9]	167	5.2 [4.8; 5.8]	5.0 [4.6; 5.5]	6.9 [5.5; 9.0]	21	5.2 [5.0; 8.0]	5.2 [4.9; 6.7]
HbA1c (%)	5.8 [5.5; 6.5]	166	5.3 [5.0; 5.7]	5.2 [4.9; 5.5]	6.2 [6.0; 7.3]	21	5.8 [5.4; 6.8]	5.5 [5.2; 6.2]
FPI (mlU/l)	20.2 [12.9; 31.6]	108	8.2 [6.6; 9.2]	6.3 [3.9; 10.2]	27.5 [22.9; 33.5]	14	11.6 (mean)	8.3 [4.6; 11.1]
HOMA-IR	5.2 [3.3; 9.7]	108	2.2 [1.3; 3.0]	1.5 [0.8; 2.5]	8.1 [6.5; 12.8]	14	3.6 (mean)	1.9 [1.0; 3.4]
Total cholesterol (mmol/l)	5.0 ± 1.1	168	4.1 ± 0.9	4.2 ± 0.7	4.6 ± 1.0	21	4.5 ± 1.0	4.7 ± 1.0
HDL-cholesterol (mmol/l)	1.2 ± 0.4	168	1.2 ± 0.4	1.5 ± 0.4	1.1 ± 0.3	21	1.0 ± 0.3	1.3 ± 0.3
LDL-cholesterol (mmol/l)	3.1 ± 1.0	168	2.4 ± 0.7	2.4 ± 0.6	2.9 ± 0.9	21	2.9 ± 0.9	2.9 ± 0.9
Triglycerides (mmol/l)	1.5 [1.2; 2.0]	168	1.2 [0.9; 1.5]	1.0 [0.8; 1.3]	1.6 [1.3; 2.6]	21	1.5 [1.3; 1.9]	1.1 [0.9; 1.5]
eGFR CKD-EPI (ml/min per 1.73 m^2)	91.3 ± 23.5	167	94.8 ± 19.1	95.0 ± 18.8	99.8 ± 20.9	21	98.1 ± 22.5	99.3 ± 23.7
AST (U/l)	27.0 [22.8; 34.8]	167	30.0 [24.6; 39.3]	25.2 [21.6; 30.6]	22.8 [19.8; 31.2]	21	25.8 [20.4; 34.8]	19.8 [17.9; 25.0]
ALT (U/l)	29.4 [21.3; 39.9]	168	30.0 [21.6; 41.4]	21.6 [17.4; 28.8]	30.0 [22.8; 48.0]	21	33.0 [17.4; 34.8]	16.5 [13.4; 20.7]
CRP (mg/l)	8.0 [4.0; 15.5]	167	3.3 [1.3; 8.6]	1.4 [0.6; 4.3]	11.3 [6.8; 13.3]	21	7.2 [4.8; 13.8]	4.9 [1.6; 6.3]
Leucocytes (x109/l)	8.1 ± 2.2	168	7.2 ± 1.9	6.7 ± 1.7	8.8 ± 2.7	21	8.3 ± 2.6	7.1 ± 2.0
T2D status (yes/no)	80/85	165	27/89	14/105	11/10	21	08/13	07/14
TWL (%)			17.5 ± 4.2	29.5 ± 7.8			18.2 ± 4.4	29.8 ± 10.1

Abbreviations: BMI: body mass index, WHR: waist-to-hip ratio, TFM: total fat mass, BP: blood pressure, FPG: fasting plasma glucose, HbA1c: glycated haemoglobin, FPI: fasting plasma insulin, HOMA-IR: homeostatic model assessment of insulin resistance, HDL: high-density lipoprotein, LDL: low-density lipoprotein, eGFR CKD-EPI: estimated glomerular filtration rate, AST: aspartate aminotransferase, ALT: alanine aminotransferase, CRP: c-reactive protein, IL6: interleukin 6, TWL: total weight loss in %. All normally distributed variables as mean ± standard deviation, others as median [25. percentile; 75. percentile]. All individuals with FGF21 measurement at baseline were included. n: Number of individuals included.

Table 2: **Characteristics of individuals undergoing Roux-En-Y gastric bypass (RYGB) and vertical sleeve gastrectomy (VSG).**

processes. To get insights into the biological processes, the analytes within one module may be involved in, the analytes of each module were subjected to enrichment analyses using clusterProfiler and Gene Ontology Biological Processes (GO BPs) from MSigDB as previously described[24] (Tables S6–S9, 10.5281/zenodo.13730671). Significant terms (BH-adjusted $p \leq 0.05$) were identified, and the top two enriched terms per module visualized, which are the ones most analytes within the module are involved in. To get information on the conditions affecting these biological processes, the correlation of modules with FGF21 levels, total fat mass loss, weight loss percentage, and T2D remission was assessed.

Statistics

Statistical analyses were conducted using R 3.6.1 and SPSS V.25. A detailed overview of objectives, relevant analyses, outcome variables and corresponding sample for each results section can be found under Table S10. In brief, the following analyses were performed in the cross-sectional setting in the maximum available sample size for each analyte: Kruskal–Wallis test for multiple group comparisons and Mann–Whitney U test for two-group comparisons. Categorical data were analysed using the Chi-square test. Non-parametric partial correlation was used to adjust correlations. Feature selection was conducted using Boruta[28] to identify key variables influencing baseline FGF21 levels, which uses a random forest algorithm to establish the feature importance score by comparing its relevance to that of randomly generated features.

In the longitudinal metabolic surgery subgroup, changes of continuous variables over time were assessed using linear mixed effect models with participants as random effects and timepoints and surgery (as well as their interaction) as fixed effects (*outcome variables*: FGF21, AST, ALT, BMI, CRP, GGT, HOMA-IR, triglycerides, visceral fat rating). Post hoc analyses to compare two groups were conducted using a pairwise Wilcoxon rank-sum test. Results were further validated in participants with data across all three timepoints using Friedman's ANOVA for overall assessment of significance over timepoints with a pairwise Wilcoxon signed-rank test for dependent samples. To assess whether surgery type impacts FGF21 differently, linear mixed-effects model was constructed, specifying FGF21 levels as *an outcome variable* and considering surgical

procedure, timepoint, their interaction as predictors, and participants as random effects. This model indicated no significant impact of the surgical procedure or its interaction with timepoint ($p_{surgery}$ = 0.72, $p_{time\text{-}point}$ = 0.003, $p_{interaction}$ = 0.93), allowing us to combine VSG and RYGB data in further analyses.

Stepwise linear regression with backward elimination was performed to determine the predictive value of weight loss and FGF21 levels for insulin resistance shortly after surgery. All predictors (%TWL, FGF21 and BMI at baseline) were included in the initial regression model followed by a stepwise removal of a predictor, if no statistically significant contribution to prediction of the *outcome variable* (HOMA-IR after three months) was detected. Backward elimination was used to avoid suppressor effects, which are more likely in forward elimination.

The area under the curve (AUC) was computed using the trapezoidal rule on the empirical ROC curve to determine how accurately FGF21 baseline levels distinguish between T2D remission and non-remission 12 months post-surgery (*outcome variable*) and how accurately the FGF21 change score at three months predicted weight loss response groups (*outcome variable*: poor and good responders according to %TWL 12 months post-surgery) with pROC.[29] For this aim, FGF21 change score was calculated as the difference between three-month and baseline-FGF21 levels. We employed a linear mixed-effects model to investigate the relationship between changes in FGF21 over time and other metabolic variables. The model included FGF21 levels as the *outcome variable*, metabolic variables (iterated over, list of variables in Table S11), and an interaction between surgery and timepoint as fixed effects, with participants as random effects. To understand the short-term connection of these variables to FGF21 changes, Spearman's rank correlations were calculated for the FGF21 change score at three months with the changes in other metabolic variables from baseline to three months after surgery (Table S16). Additionally, a sensitivity analysis was performed by excluding the smaller VSG subgroup and conducting the correlations in the RYGB group alone to assess the consistency of the results (Table S16).

We conducted multivariable linear regression to identify predictors of HOMA-IR, weight loss, and fat mass loss one year after surgery (*outcome variables* of the regression models, respectively: HOMA-IR at 12 months post-surgery, weight- and fat mass loss 12 months post-surgery, predictor variables included FGF21 three- and 12-months change score, calculated as the difference between 3 months or 12-month and baseline-FGF21 levels respectively and variables listed under Tables S19–S21). To determine the most important predictors, we used recursive feature elimination. All the significantly associated variables from the multiple linear regression step were included in one model. Before that, we removed any predictor variables with high multicollinearity by excluding those with a high variance inflation factor. To standardize the model features, we transformed the data by centring and scaling it, which can improve model performance and feature importance assessment.

Causal mediation analysis was conducted to determine whether free fatty acids (FFA) concentration causally influences post-surgery FGF21 changes (direct effect of FFA on FGF21) and to assess if this effect is mediated by the liver (effect of FFA on FGF21 via ALT). In this analysis, FGF21 serves as the *outcome variable*, FFA as the exposure, and ALT as the mediator. Variables were log-transformed prior to the analysis, which was executed using the mediation package[30] with 500 nonparametric bootstrapping simulations. p values < 0.05 were considered significant and where necessary, corrected for multiple testing according to Benjamini Hochberg to account for the false discovery rate at a significance level of p_FDR<0.05.

Role of funders

The funders of this study had no role in data collection, study design, participant recruitment, analysis, writing or interpretation, or any aspect pertinent to the study.

Results

FGF21 is associated with cardiometabolic burden and is driven by circulating leptin

We first aimed to probe the links between FGF21 levels and cardiometabolic disease. FGF21 emerged as a significant marker of cardiometabolic and cardiovascular risk, as evidenced by its correlation with the Framingham ASCVD 10-year risk score (rho = 0.39, p < 0.001, spearman's rank correlation, Fig. 1a). FGF21 levels also showed specific associations with individual cardiovascular risk factors and disease severity: Notably, elevated FGF21 levels reflected more closely increased central adiposity (WHR, visceral fat mass) rather than total fat mass, and increased insulin resistance, subclinical inflammation (leucocyte counts, C-reactive protein [CRP]), liver enzymes, as well as blood pressure (Fig. 1b). These correlations persisted after adjustments for T2D status, age, BMI, and estimated glomerular filtration ratio (eGFR) (Table S12). The association between FGF21 levels and the severity of metabolic disease was further substantiated by its association with microalbuminuria, as a marker of early metabolic kidney damage and the number of antidiabetic, antihypertensive, and lipid-lowering medications prescribed (Fig. 1b, Table S13).

To understand the relative importance of the many related features in predicting circulating FGF21, we performed recursive feature elimination on extensive clinical data and circulating proteins. This analysis

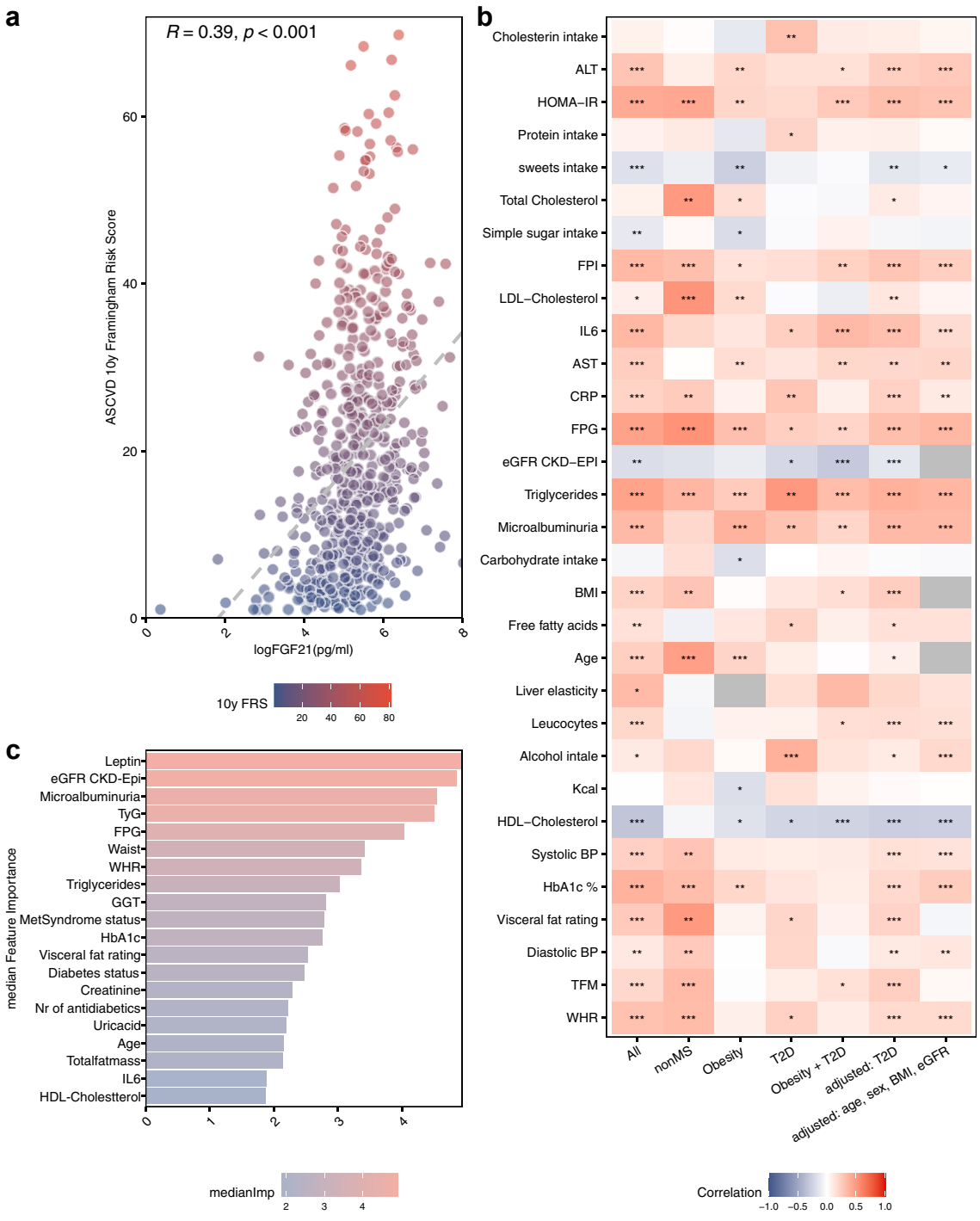

Fig. 1: **FGF21 along BMI and metabolic impairment spectrum**. (**a**) Spearman's rank correlation between FGF21 serum levels and the Framingham ASCVD 10-year risk score (10y FRS). Point colours represent an escalating 10y FRS, transitioning from deep blue to a richer red. (**b**) Spearman's rank correlations illustrate the relationship between metabolic parameters and circulating FGF21. The direction of correlation is represented by color—positive (red) and negative (blue) with the hue intensity denoting the magnitude of the correlation effect. Significance is indicated by asterisks: *, $p \leq 0.05$; **, $p \leq 0.01$; ***, $p \leq 0.001$; no asterisks-not significant. grey coloured field—not detectable. (**c**) Recursive feature elimination highlighting the main factors influencing FGF21 serum levels and their feature importance. ***Abbreviations***: ALT (alanine aminotransferase), HOMA-IR (homeostatic model assessment of insulin resistance), FPI (fasting plasma insulin), IL6 (interleukin 6), AST (aspartate aminotransferase), CRP (c-reactive protein), FPG (fasting plasma glucose), eGFR (estimated glomerular filtration rate), BMI (body mass index), Kcal (estimated Kilocalories intake), HDL (high-density lipoprotein), HbA1c (glycated haemoglobin), BP (blood pressure), TFM (total fat mass), TyG (triglyceride glucose index), WHR (waist-to-hip ratio), GGT (gamma-glutamyl transferase), MetSyndrome (metabolic syndrome).

highlighted kidney dysfunction, central adiposity, glucose control, and liver enzymes as key selected features. Notably, circulating leptin emerged as the top predictor, implying an association between FGF21 and AT. These findings underscore the relationship between FGF21 and metabolic dysfunction, as well as organ impairments associated with central adipose tissue distribution, particularly in kidney and liver function (Fig. 1c).

Circulating FGF21 links to AT-traits reflecting lipid dysmetabolism and fibro-inflammatory pathways

As adipocytes are the main source of leptin,[31] the top predictor of FGF21, we explored the connections between white adipose tissue (WAT) traits and circulating FGF21 levels: Higher circulating FGF21 levels associated with increased adipocyte-size and reduced adipocyte-counts in both subcutaneous (sc) and visceral (vis)AT. Elevated circulating FGF21 covaried with increased macrophage infiltration in visAT, pointing to an inflammatory state that uniquely correlated with increased liver GGT, a marker of liver dysfunction (Fig. 2a).

Our analysis further extended to specific transcripts and proteins within scAT and visAT, revealing a co-regulation with circulating FGF21 (Fig. 2b, Figure S1): Key features consistently associated across both ATs included transcripts and proteins involved in lipid metabolism pathways such as CDP-diacylglycerol synthase 2 (*CDS2*), BCL3 Transcription Coactivator (*BCL3*).[32] Notably, adaptor-related protein complex 2 subunit mu 1 (*AP2M1*),[33] and lysosomal associated membrane protein 2 (*LAMP2*)[34] were consistently linked with FGF21 levels in both ATs, reinforcing the notion that FGF21 impacts lipid processing and storage mechanisms (Fig. 2c). Additional consistent features across transcriptome and proteome included alcohol dehydrogenase 1B (*ADH1B*), phosphoserine aminotransferase 1 (*PSAT1*), and *CD248* relating to fibro-inflammatory pathways.

Our analysis also revealed that in scAT, FGF21 associated with increased vesicle trafficking, intracellular transport, remodelling, reduced ubiquitin-proteasome pathway, and modified cell–cell interactions, as well as with lower *fibroblast growth factor receptor 1* (*FGFR1*) expression (rho = –0.44, p = 0.04, spearman's rank correlation). In visAT, FGF21 correlated positively with several transcripts and proteins relating to autophagy, phospholipid metabolism, and mitochondrial dysfunction, as well as with the marker of inflammation serum amyloid A1 (SAA1). However, no direct correlation was observed between FGF21 and AT-fibrosis, as indicated by the histological FAT-score in either AT depots (Table S14). These results underscore histological and molecular underpinnings of WAT dysfunction associated with FGF21 levels, emphasizing a distinct connection between visAT inflammation and liver dysfunction and pathways related to stress response, immunomodulation, insulin resistance, lipid raft signalling and tissue remodelling.

FGF21 trajectory in metabolic surgery indicates liver catabolic response in the short-term

Metabolic surgery is recognized for its impact on cardiometabolic improvement,[7,13] despite existing debate concerning its impact on FGF21.[7] We hence investigated FGF21 dynamics post-surgery. Overall, surgery led to substantial weight loss, improved insulin sensitivity, lipid profiles, and reduced inflammation, although with notable variability (Fig. 3a, Table 2). Among 86 individuals with T2D at baseline, 57 achieved remission but individuals with or without remission did not differ in FGF21 levels at baseline, three or 12 months (Table S15).

Circulating FGF21 levels initially increased at three months post-surgery, before declining below baseline levels at the 12-months mark (Fig. 3b). The investigation of their short-term dynamics identified liver enzyme trajectories (Figure S2), and serum albumin as the only features significantly covarying with FGF21 change scores at three-months post-surgery after correction for multiple testing. While FGF21 and liver enzymes changed in the same direction (Fig. 3a), higher increases of FGF21 at three months were correlated with lower serum albumin (Table S16). Importantly, sensitivity analyses revealed consistent results when the smaller VSG subgroup was excluded with a slightly reduced power for correlation analyses (Figure S3, Table S16). Together, these results indicate that higher early increases in FGF21 were associated with a more pronounced liver response to catabolism in metabolic surgery.

FGF21 dynamics predict weight loss but not improvement of insulin sensitivity at 12-months

Given the conflicting reports on the effects of metabolic surgery on FGF21 and its subsequent associations with metabolic improvements,[7,19] along with the modest efficacy of FGF21 analogues in controlling glycaemia,[7] we explored the relationship between FGF21 and surgical outcomes: The reduction of FGF21 from baseline to 12 months paralleled improvements in metabolic parameters including glucose, lipid metabolism, and inflammation (Fig. 3a), with the 12-months CVD-risk inversely relating to the FGF21-decrease over 12-months ($rho_{Framingham}$ = –0.190, p = 0.021, spearman's rank correlation, Figure S4). However, post-surgery FGF21 levels maintained their positive association with CVD risk similar to baseline levels ($rho_{Framingham}$ = 0.41, p < 0.001, spearman's rank correlation).

Remission of T2D was observed in most patients with good responsiveness in terms of weight loss, while

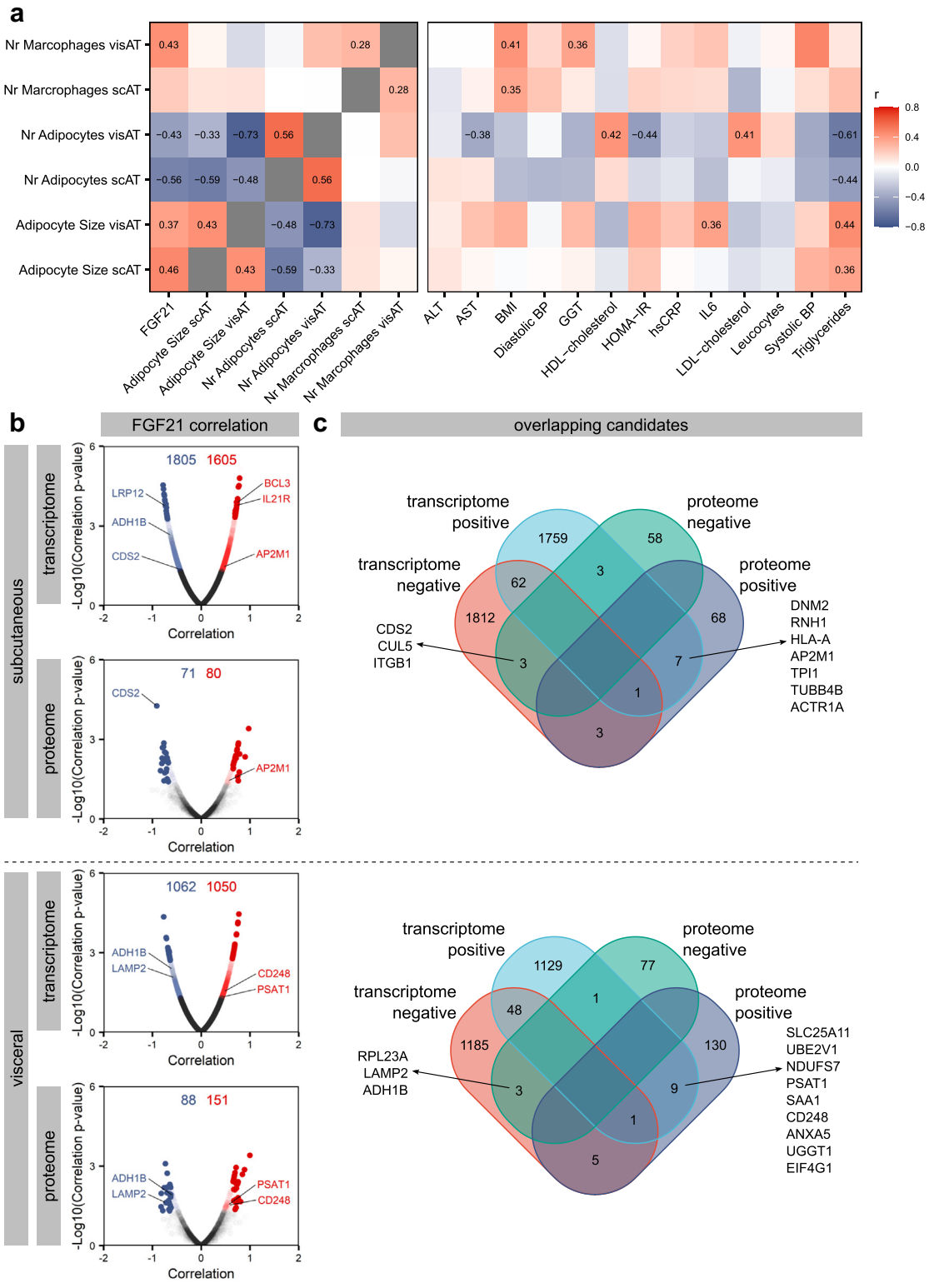

Fig. 2: **Correlation of FGF21 levels with AT characteristic**s. (**a**) Spearman's rank correlations between circulating FGF21 levels and histological adipose tissue (AT) characteristics, alongside metabolic markers. Only tiles having significant correlations ($p \leq 0.05$) are labelled with their

only a third of poor responders experienced T2D remission (Table S17).

To investigate the effect of weight loss vs FGF21 changes on insulin resistance improvement, stepwise linear regression analysis with backward elimination was performed (Table S18). The decrease in HOMA-IR at three months was best predicted by baseline FGF21 and BMI (explaining 45.7% of HOMA-IR improvement, step 2: outcome variable: HOMA-IR at three months, predictor variables: baseline BMI and FGF21, corrected $r^2 = 0.457$). The inclusion of %TWL did not enhance the model's predictive ability (step 1: outcome variable: HOMA-IR at three months, predictor variables: %TWL, baseline BMI and FGF21, corrected $r^2 = 0.441$). This suggests that lower baseline FGF21 levels, indicative of better pre-surgery metabolic status, predict early improvements in insulin resistance after surgery, irrespective of weight loss. However, baseline FGF21 modestly predicts T2D remission at one year (AUC = 0.6, accuracy = 0.30). In line with this, the FGF21 change score at three or 12 months did not significantly predict HOMA-IR at 12 months in change score regression (with or without baseline correction) or recursive feature elimination (Table S19 and 10.5281/zenodo.13730671).

On the other hand, FGF21 dynamics significantly related to weight and fat loss outcomes: higher FGF21 change scores three-months post-surgery were significantly higher in good responders (%TWL ≥20%) vs poor responders (%TWL <20%) (Fig. 3c) and effectively differentiated between these two groups (AUC 0.73, accuracy of 0.66). In other words, if two random individuals from our cohort are chosen, one poor and one good responder, the probability of FGF21 change score at three months being higher in the good responder is 73%. Similarly, FGF21 change score at three-months was a significant predictor for both weight and fat loss at 1 year as continuous variables (Tables S20, S21, 10.5281/zenodo.13730671).

AT architecture relates to FGF21 dynamics and T2D remission post-metabolic surgery

Because characteristics of adipose tissue seem to partly dictate FGF21 levels, we aimed to decipher WAT processes linked to observed FGF21 changes post-metabolic surgery. For this, we conducted WGCNAs on transcriptomes and proteomes from sc- and visATs, identifying modules of co-abundant transcripts and proteins relating to FGF21 levels post-surgery (Fig. 4).

In the visAT transcriptome (Fig. 4a, Table S7), the yellow module showed a negative correlation with T2D remission, although no pathways were significantly enriched in this module. In contrast, three modules showed significant correlations with FGF21 levels and T2D remission in the visAT proteome (Fig. 4b, Table S9). Among these, the black module, which negatively correlated with FGF21 levels at both three and 12 months as well as with T2D remission, enriched for pathways involved in central carbon and fatty acid metabolism. Meanwhile, the turquoise module, alongside showing similar enrichments, also enriched for processes related to inflammatory responses and was related to higher FGF21 levels but reduced T2D-remission rates.

In the scAT transcriptome (Fig. 4c), the tan module, related to growth and chemotactic processes (Table S6), positively associated with T2D remission, and negatively with 12-month FGF21 levels. Moreover, the scAT proteome (Fig. 4d), showed most associations to FGF21 levels, including at three-months, and T2D remission. In this analysis, modules related to immune responses and oxidant detoxification (green and black modules) showed a strong positive correlation with FGF21 levels at three months and T2D remission (rho = 0.77, p = 0.030), linking this desired outcome to the mentioned processes in scAT at baseline (Table S8). These results underscore the relationship between adipose tissue transcriptomic and proteomic profiles and changes in FGF21 levels over time following surgery

corresponding effect size. Correlation direction is denoted by colour: positive correlations are red and negative ones are blue, with the depth of the hue reflecting the strength of the correlation. (**b**) Correlation assessments with circulating FGF21 were conducted for each transcript and protein derived from subcutaneous adipose tissue (scAT) or visceral adipose tissue (visAT). Candidates demonstrating significant positive correlations ($p \leq 0.05$) are presented in red, while those showing negative correlations are illustrated in blue. The cumulative count of these significant candidates is provided. Pertinent candidates are clearly marked. For clarity, the top 25 and bottom 25 candidates in terms of correlation strength are rendered opaque. (**c**) Venn diagram showcasing the overlap between transcripts and proteins that significantly correlate with circulating FGF21 either positively or negatively (termed transcriptome/proteome negative or positive). ***Abbreviations***: ALT (alanine aminotransferase), AST (aspartate aminotransferase), BMI (body mass index), BP (blood pressure), GGT (gamma glutamyl transferase), HDL (high-density lipoprotein), HOMA-IR (homeostatic model assessment of insulin resistance), CRP (c-reactive protein), IL6 (interleukin 6), LDL (low density lipoprotein), CDS2 (CDP-Diacylglycerol Synthase 2), CUL5 (Cullin-5), ITGB1 (Integrin Subunit Beta 1), DNM2 (Dynamin 2), RNH1 (Ribonuclease/angiogenin Inhibitor 1), AP2M1 (Adaptor Related Protein Complex 2 Subunit Mu 1), HLA-A (Major Histocompatibility Complex, Class I, A), TPI1 (Triosephosphate Isomerase 1), TUBB4B (Tubulin Beta 4B Class IVb), ACTR1A (ARP1 Actin-Related Protein 1 Homolog A, Centractin Alpha), RPL23A (Ribosomal Protein L23a), LAMP2 (Lysosomal Associated Membrane Protein 2), ADH1B (Alcohol Dehydrogenase 1B (Class I), Beta Polypeptide), SCL25A11 (Solute Carrier Family 25 Member 11), UBE2V1 (Ubiquitin Conjugating Enzyme E2 V1), NDUFS7 (NADH:Ubiquinone Oxidoreductase Core Subunit S7), PSAT1 (Phosphoserine Aminotransferase 1), SAA1 (Serum Amyloid A1), CD248 (Endosialin), ANXA5 (Annexin A5), UGGT1 (UDP-Glucose Glycoprotein Glucosyltransferase 1), EIF4G1 (Eukaryotic Translation Initiation Factor 4 Gamma 1).

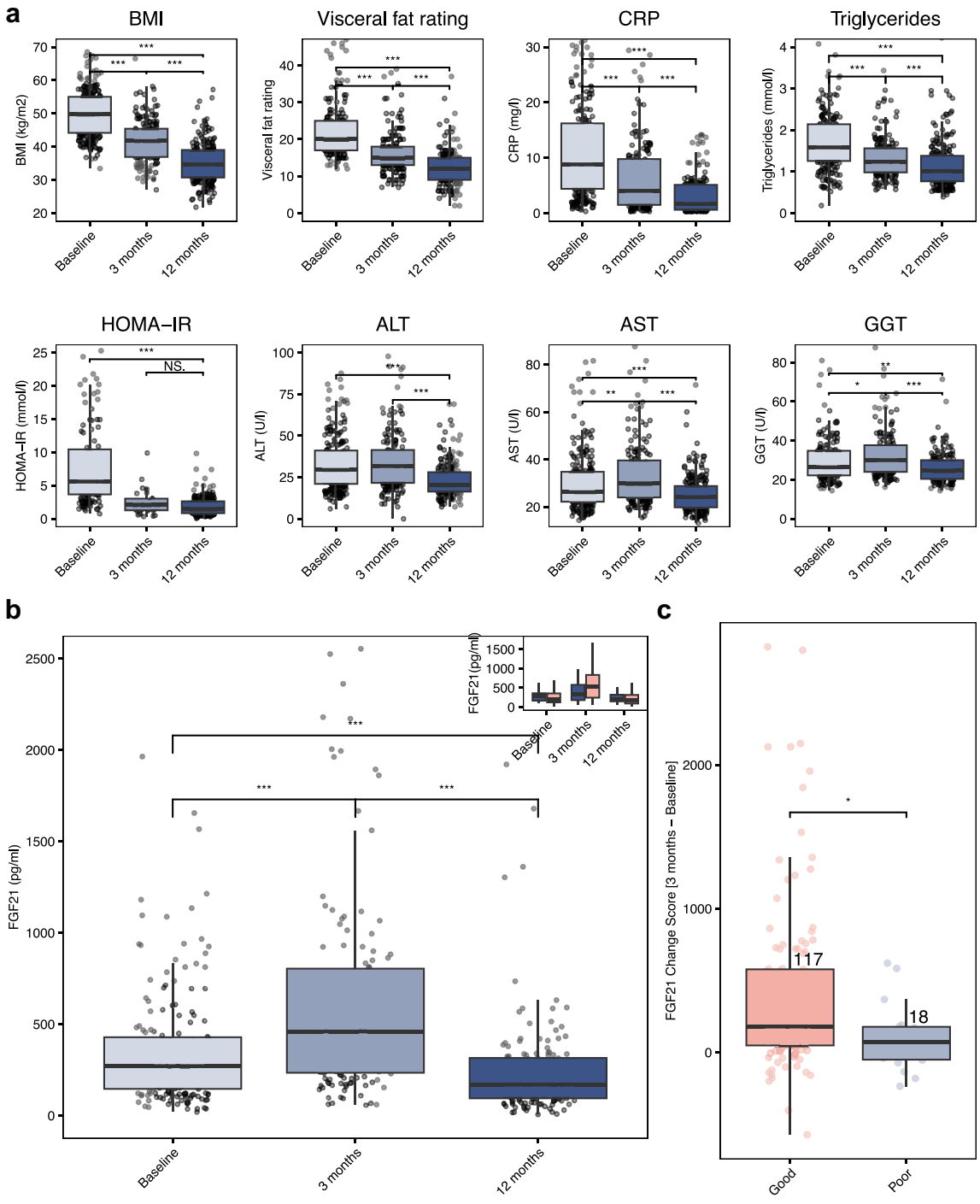

Fig. 3:* FGF21 dynamics following metabolic surgery**. (**a**) Longitudinal changes following metabolic surgery in BMI (kg/m^2), visceral fat rating, CRP (mg/l), triglycerides (mmol/l), HOMA-IR, ALT (U/l), AST (U/l), and GGT (U/l) at baseline, three, and 12 months for up to 189 individuals. Statistical analyses: Friedman's ANOVA for overall differences. (**b**) Longitudinal changes in FGF21 serum concentration (pg/ml) from before to 12 months post-surgery using the same statistical test as in (a). Inset boxplot differentiates results by response type: poor (blue, n = 18) and good (light pink, n = 122) responders. (**c**) Comparison of FGF21 change score at three months between poor (n = 18) and good responders (n = 122) assessed using Mann–Whitney U test. Significance is indicated by asterisks: *-p ≤ 0.05, **-p ≤ 0.01, ***-p ≤ 0.001. ***Abbreviations: BMI (body mass index), CRP (c-reactive protein), HOMA-IR (homeostatic model assessment of insulin resistance), ALT (alanine aminotransferase), AST (aspartate aminotransferase), GGT (gamma glutamyl transferase).

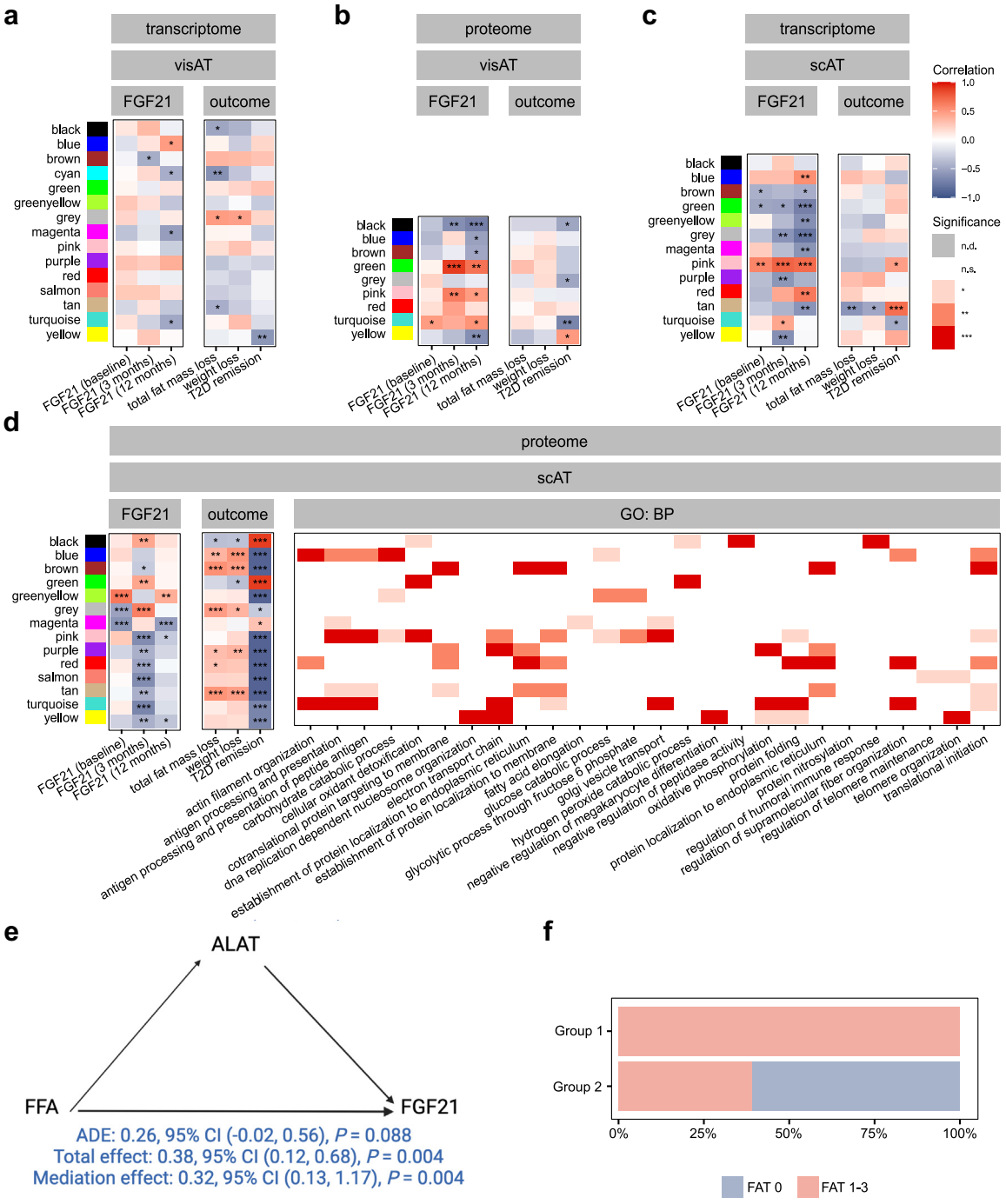

Fig. 4: **Correlation of clusters of transcripts and proteins from visAT and scAT with metabolic outcomes after metabolic surgery**. WGCNA was applied to transcripts and proteins from baseline visAT (**a, b**) and scAT (**c, d**) The obtained modules of co-abundant transcripts and proteins were correlated with FGF21 levels and the selected metabolic outcomes. Correlation direction is denoted by colour: positive correlations are red and negative ones are blue, with the depth of the hue reflecting the strength of the correlation. To get insights into the processes mirrored by the modules, enrichment analyses were conducted with all candidates assigned to one module. The top 2 enriched biological processes (BPs) from the Gene Ontology (GO) database are shown for the scAT proteome (**d**, right panel). The significance of enrichment is reflected by the intensity colour. (**e**) Mediation analysis between FFA, ALT as a marker of liver response and FGF21. The total effect of FFA on FGF21 (model including FFA and ALT) was significant, with the average causal mediated effect (ACME) (the effect of the ALT alone on FGF21) being significant, while the average direct effect and hence unmediated of FFA (ADE) was not significant. FFA influx hence only increases FGF21 when it

and T2D remission. They further suggest that the metabolic processes influencing T2D remission post-surgery are predominantly mediated at the protein level, potentially through post-translational modifications that affect protein aggregation, degradation, and release into surrounding tissues.

AT-liver axis mediates FGF21 levels in metabolic disease and surgery

Using integration of AT-omics, we showed that early post-surgery increase in FGF21 associated with both visAT and scAT proteome. Also, the change in FGF21 in the short-term was mainly linked to increased markers of liver health and function, reduced albumin, and more importantly predicted fat mass loss. As a result, we wondered whether overlapping characteristics of insulin resistance and AT lipolysis were connected to FGF21 increases via the liver.

In this context, we explored whether free fatty acids (FFA), elevated due to AT insulin resistance and lipolysis[35] could serve as a putative link between visAT and hepatic production of FGF21. A causal mediation analysis was employed to assess the direct effect of FFA concentration on post-surgical changes in FGF21 levels and to examine whether this effect is mediated by liver response, specifically through changes in ALT levels. In this analysis, FGF21 serves as the outcome variable, FFA is the exposure, and ALT acts as the mediator (Fig. 4e, Table S22). The total effect of FFA on FGF21 was significant (total effect = 0.38, p = 0.004), indicating a robust association between FFA concentrations and FGF21 levels. Notably, 32% of this effect was mediated by the liver, as evidenced by changes in ALT (p = 0.004), suggesting that liver function plays a significant role in how FFA influence FGF21 levels. Furthermore, the average causal mediated effect (ACME) by ALT alone was significant (ACME: 0.12, p < 2e-16), highlighting a strong mediation pathway through the liver. In contrast, the average direct effect (ADE) of FFA on FGF21, not mediated by liver enzymes, was statistically nonsignificant (ADE: 0.12, p = 0.088, Fig. 4e). Similar results were obtained when GGT was used as a mediator instead of ALT (Table S22), reinforcing the importance of the liver's role in this metabolic process.

Since AT is the main source of FFA release, we explored whether FFA can be linked to AT-characteristics and therefore to metabolic outcomes. FFA levels were mainly positively associated with fat mass loss and negatively with visAT fibrosis scores (rho = 0.17 and –0.31; p = 0.020 and 0.030, respectively, spearman's rank correlation). Accordingly, stratifying individuals according to their fat mass loss showed that those with less than 40% fat mass loss had a more significant degree of fibrosis compared to those with fat mass loss of ≥50% (Fig. 4f).

Discussion

This study aimed to identify factors associated with serum FGF21 levels across a large cross-sectional cohort representing a range of metabolic disease severity. Additionally, it examined these levels in a longitudinal subset of individuals undergoing metabolic surgery, focusing on the relationship between FGF21-dynamics and metabolic improvements. We explored AT phenotypes, including histology, transcriptomics, and proteomics, to understand their potential interplay with FGF21 in surgical outcomes. Our research first confirms that elevated levels of FGF21 are linked with central adiposity, insulin resistance, systemic inflammation, and increased cardiometabolic risk.[7,36] Intriguingly, circulating leptin emerged as the top feature predicting circulating FGF21, suggesting a potential link between AT and FGF21.[31] Indeed, we found a significant correlation between circulating FGF21 and adipocyte size in both sc- and visAT and accordingly with AT lipid storage (e.g., *CDS50*[37]). Importantly, we observed a unique association between circulating FGF21 with inflammatory SAA1 in visAT and with resident macrophages, which in turn, were linked to raised liver enzymes in our cohort. In line with this, several features of visceral-adiposity-linked impairment including indices of insulin resistance (TyG-index) and elevated liver markers were among the top variables in the FGF21-prediction model in our study. Indeed, ectopic fat accumulation, specifically visceral, and intrahepatic fat, haven been shown to be associated with serum FGF21 levels in T2D.[38] The relevance of visAT towards FGF21 levels in T2D may partly be explained through a lower expression of genes leading to reduced FGF21 signalling (such as FGFR1, β-klotho) in visAT compared scAT,[38] suggesting an FGF21 resistance of visAT in T2D as a basis for the higher FGF21 serum levels.

Interestingly, despite the observed weight loss and metabolic improvements post-surgery, we noted an increase in FGF21 levels at the three-months mark. This peak coincided with an increase in liver enzyme levels and a decrease in circulating albumin at the same timepoint. This finding, along with the evidenced importance of liver enzymes in predicting FGF21 levels at baseline suggest that physiological changes linked to both insulin resistance in central adiposity, AT-lipolysis,

elicits a response in the liver. Total effect = ADE + ACME. (**f**) Fraction of individuals with fibrosis (FAT score 1–3) and without fibrosis (FAT score 0) in scAT within individuals with <40% fat mass loss (group1, n = 9) and individuals with ≥50% fat mass loss (group 2, n = 25) (Chi-square analysis). Significance is indicated by asterisks: *, p ≤ 0.05; **, p ≤ 0.01; ***, p ≤ 0.001; n.s., not significant; n.d., not detectable. ***Abbreviations***: scAT (subcutaneous adipose tissue), visAT (visceral adipose tissue), FFA (free fatty acids), T2D (type 2 diabetes), ALT (Alanyl aminotransferase), ADE (average direct effect), ACME (average causal mediated effect), FAT score (fibrosis score of adipose tissue).

and increased catabolism may disproportionally affect the liver as the primary link with FGF21. VisAT fibrosis, on the other hand, shown to reduce lipolysis,[39] was negatively linked to fat mass loss and FFA in our study, suggesting that the increase in FGF21 at three-months could be an indirect indicator of a responsive AT, with maintained capacity for lipolysis. Importantly, the link between FFA and FGF21 seemed to be entirely dependent on the liver's response as indicated by mediation analysis.

These results align with the understanding that FFAs, which increase due to the insufficient insulin-dependent inhibition of AT-lipolysis in states of insulin resistance, are strong determinants of FGF21 levels.[7] Furthermore, the acute rise in FFAs following metabolic surgery, leading to increased hepatic activation of PPAR-α,[40] the key regulator of hepatic FGF21,[41] underscores the dynamic interplay between AT and liver response in the pathophysiology of obesity and weight loss.

The post-surgical increase in FGF21 could also relate to the central effects of food and protein restriction. This is partly supported by the negative correlation observed between caloric intake and FGF21 levels in our cohort, akin to FGF21 increases seen in extended fasting scenarios.[7] Notably, FGF21 can cross the blood–brain barrier, and its levels in cerebrospinal fluid have been correlated with obesity, fat mass, and insulin resistance.[42] A low-protein, high-carbohydrate diet has been shown to significantly elevate FGF21 under controlled food intake conditions, with such increases predicting lower weight gain after a six-months follow-up in free-living conditions.[43] Consistently, we observed that a less pronounced increase in FGF21 after three months was associated with lower degrees of weight and fat loss. This outcome may be related to the central role of FGF21 in glutamatergic signalling within the ventromedial hypothalamus, which suppresses food intake[44] and enhances leptin action,[45] thereby reducing body weight. However, our study lacks post-surgery dietary intake data to fully substantiate this hypothesis.

Overall, our results are in line with several studies showing an increase of FGF21 after metabolic surgery or caloric restriction in the short term,[16,17,46] and a reduction around the one year mark.[17,47] However, the results are in contrast with weight loss studies that either show that FGF21 is reduced in caloric restriction or report non-significant decreases of FGF21 one year after surgery.[16,19] It is important to note that the divergent evidence regarding FGF21 levels after weight loss may be attributed to several factors including diet composition, individual variability and specific intervention protocols: Variations in protein vs carbohydrate intake significantly influence FGF21 levels and diet explains over half the amount of variance observed in FGF21 levels making it the most important exogenic determinant.[48] Additionally, genetic predispositions—such as single nucleotide polymorphisms in or near the FGF21 gene—affect individual food preferences, body composition and FGF21 levels.[49] Discrepancies also arise from the diversity in study protocols, including sex distribution, sample size impacting power of the study, the duration of fasting, types of metabolic surgery, and timing of FGF21 measurements capturing different metabolic responses.[7] Further complexity is added by the metabolic health status of individuals studied: Studies often do not distinguish between metabolically healthy and metabolically unhealthy obesity (MUHO), which can significantly influence FGF21 levels and dynamics. FGF21 levels are higher in MUHO and liver fat content is the strongest determinant of hepatic FGF21 production and circulating FGF21 levels independent of BMI.[50,51] Accordingly, studies should be read with care and future research should focus on standardizing dietary and surgical protocols with detailed reporting, and longitudinally tracking FGF21 levels across genetically diverse groups with in-depth assessments of metabolic health.

Considering recombinant FGF21's effectiveness in reducing weight in rodent models of obesity,[7,13,52] and mixed outcomes of FGF21 analogues on glycaemic control,[13,52] we investigated the relationship between FGF21 and metabolic as well as anthropometric outcomes following metabolic surgery. Interestingly, changes in HOMA-IR at one year were not directly related to changes of FGF21 levels at either three or 12 months. However, an initial lower FGF21 level predicted a short-term improvement in HOMA-IR, aligning with evidence that lower metabolic burden before surgery is associated with higher remission rates of T2D.[53] This suggests that improvements in HOMA-IR at 12 months may be largely secondary to weight loss.

Furthermore, changes in FGF21 levels at three months were predictive of reductions in weight and fat mass at one year, in line with a recent adequately powered study.[54] Whether the initial increase in FGF21 contributes to fat mass loss and subsequent metabolic and inflammatory improvements at 12 months remains speculative. Supporting this speculation is the observation that increased PPAR-α activation enhances hepatic FA oxidation, contributes to fat depot reduction, and improves metabolic and inflammatory parameters and that FGF21 induces both lipolysis and AT-beigeing leading to increased energy expenditure.[7,55] Conversely, RYGB in FGF21-KO mice induced similar weight loss as in wild-type animals, suggesting FGF21 is not essential for weight loss after metabolic surgery.[56]

Limitations

Despite our unique integrative multi-omics approach providing numerous insightful observations of interest, our study has limitations: While we demonstrate a potential causal connection between AT and FGF21 via the

liver, limitations of the employed causal mediation analysis frame include the possibility of residual confounding as not all variables influencing FGF21 and liver enzymes may be accounted for. Moreover, interpretations are contingent upon the accuracy and stability of liver enzymes as mediators, which may vary across different populations or conditions. Additionally, we do not know how much AT may contribute to circulating FGF21 after surgery. Before surgery, *FGF21*-expression in AT did not correlate with circulating FGF21 suggesting no direct contribution of AT to these levels, which is in line with previous evidence of very low FGF21-expression in scAT and visAT.[57] Moreover, while we cannot exclude that FGF21 levels and their changes after surgery are due to FGF21 resistance in AT, *FGFR1*-expression correlated negatively with circulating FGF21 levels but only in scAT. As we do not have AT biopsies from 3- and 12-months, we are unable to investigate the effect of metabolic surgery on *FGFR1*-expression in adipose tissue and conclusively discuss the aspect of FGF21-resistance.

Notwithstanding, our research uniquely integrates liver and adipose tissue data into a unified framework, revealing AT-liver crosstalk as a potential determinant of circulating FGF21 both in metabolic disease and after metabolic surgery. Additionally, we posit that visAT fibrosis can influence fatty acid availability and thus FGF21 secretion, adding a new dimension to our understanding of metabolic regulation. Within this integrated framework, endogenous FGF21 reflects liver's exposure to increased FFA: When visceral fat is increased, FFA are released through the portal system due to inadequate insulin-dependent inhibition of lipolysis leading to increased FGF21 in association with other markers of glucometabolic control. After surgery, healthier adipocytes, showcasing less fibrosis, are more lipolytic resulting in elevated levels of FFAs and FGF21, which are reflected in more favourable outcomes in weight loss, particularly when FGF21 concentrations are reduced owing to a decreased baseline rate of lipolysis after surgery. Within this specific context, short-term FGF21 change serves as a biomarker for healthier adipose tissue and a positive response to metabolic surgery, rather than acting as a primary effector of metabolic response as previously suggested by preclinical models, warranting further validation.

Contributors

M.P., I.K., L.K., R.C. have accessed and verified the underlying data and conducted the analyses presented in this manuscript. M.P., I.K., K.M., R.C. wrote the manuscript. L.M., S.T., M.G. performed histological analyses and conducted analyses of AT-fibrosis. T.K. recruited and phenotyped participants. A.D. and M.B. collected adipose tissue samples and recruited participants. M.B. is responsible for the Leipzig obesity Biobank (LOBB). M.v.B conducted AT proteomics. M.S. P.K., M.v.B., K.S. and R.C. provided funding relevant for the conduction of the study and subsequent analyses. L.M., T.S., M.G., M.B., K.S. and P.K supported the critical data interpretation and reviewed the manuscript. All authors read and approved the final manuscript.

Data sharing statement

All data generated or analysed during this study are included in this published article and its Supplementary information files. Further metadata sharing is subject to research agreement proposals and inquiries should be directed to the corresponding author.

Declaration of interests

MB received honoraria as a consultant and speaker from Amgen, AstraZeneca, Bayer, Boehringer-Ingelheim, Lilly, Novo Nordisk, Novartis and Sanofi. RC received support for attending meetings and/or travel from the National Doctoral Programme in Infection and Antibiotics (NDPIA) by The Swedish Research Council (VR, Vetenskapsrådet) and DFG (German Research Association). All other authors declare no conflict of interest. TK received two unrestricted research grants from Echosens and Canon Medical Systems.

Acknowledgements

Microarray analysis was conducted at the Core Unit DNA Technology at the Faculty of Medicine of the University Leipzig. We thank Prof. Staffan Nilsson for statistical guidance. We thank the technical team for their excellent technical support and the study participants for their support. The graphical abstract was created using Biorender.com.

This work was supported by the Deutsche Forschungsgemeinschaft (DFG, German Research Foundation) through CRC 1052, project number 209933838 and by a junior research grant by the Medical Faculty, University of Leipzig, and by the Federal Ministry of Education and Research (BMBF), Germany, FKZ: 01EO1501. Part of this work was supported by the European Union's Seventh Framework Program for research, technological development and demonstration under grant agreement HEALTH-F4-2012-305312. Funding for Helmholz Centre Research group Personal for MvB was provided by the CRC1382 and the Novo Nordisk Foundation. K.S. is grateful for funding from the Deutsche Forschungsgemeinschaft (DFG, German Research Foundation), project number 530364326. RC was supported by a Walther-Benjamin fellowship from the Deutsche Forschungsgemeinschaft (DFG, German Research Foundation).

Appendix A. Supplementary data

Supplementary data related to this article can be found at https://doi.org/10.1016/j.ebiom.2024.105458.

References

1 Busetto L, Dicker D, Frühbeck G, et al. A new framework for the diagnosis, staging and management of obesity in adults. *Nat Med*. 2024;30(9):2395–2399. https://doi.org/10.1038/s41591-024-03095-3.
2 Blüher M. Adipose tissue dysfunction in obesity. *Exp Clin Endocrinol Diabetes*. 2009;117:241–250.
3 Virani SS, Alonso A, Benjamin EJ, Bittencourt MS. Heart disease and stroke statistics—2020 update: a report from the American Heart Association. *Circulation*. 2020;141(9):e139–e596.
4 Cefalu WT, Bray GA, Home PD, et al. Advances in the science, treatment, and prevention of the disease of obesity: reflections from a diabetes care editors' expert forum. *Diabetes Care*. 2015;38:1567–1582.
5 Hanipah ZN, Schauer PR. Bariatric surgery as a long-term treatment for type 2 diabetes/metabolic syndrome. *Annu Rev Med*. 2020;71:1–15.
6 von Holstein-Rathlou S, BonDurant LD, Peltekian L, et al. FGF21 mediates endocrine control of simple sugar intake and sweet taste preference by the liver. *Cell Metab*. 2016;23:335–343.
7 Keuper M, Häring H-U, Staiger H. Circulating FGF21 levels in human health and metabolic disease. *Exp Clin Endocrinol Diabetes*. 2020;128:752–770.
8 Berglund ED, Li CY, Bina HA, et al. Fibroblast growth factor 21 controls glycemia via regulation of hepatic glucose flux and insulin sensitivity. *Endocrinology*. 2009;150:4084–4093.
9 Adams AC, Yang C, Coskun T, et al. The breadth of FGF21's metabolic actions are governed by FGFR1 in adipose tissue. *Mol Metab*. 2012;2:31–37.
10 Pereira RO, Marti A, Olvera AC, et al. OPA1 deletion in brown adipose tissue improves thermoregulation and systemic metabolism via FGF21. *Elife*. 2021;10. https://doi.org/10.7554/eLife.66519.
11 Sanyal A, Charles ED, Neuschwander-Tetri BA, et al. Pegbelfermin (BMS-986036), a PEGylated fibroblast growth factor 21 analogue, in

patients with non-alcoholic steatohepatitis: a randomised, double-blind, placebo-controlled, phase 2a trial. *Lancet*. 2019;392:2705–2717.
12 Charles ED, Neuschwander-Tetri BA, Pablo Frias J, et al. Pegbelfermin (BMS-986036), PEGylated FGF21, in patients with obesity and type 2 diabetes: results from a randomized phase 2 study. *Obesity*. 2019;27:41–49.
13 Geng L, Lam KSL, Xu A. The therapeutic potential of FGF21 in metabolic diseases: from bench to clinic. *Nat Rev Endocrinol*. 2020;16:654–667.
14 Chavez AO, Molina-Carrion M, Abdul-Ghani MA, Folli F, Defronzo RA, Tripathy D. Circulating fibroblast growth factor-21 is elevated in impaired glucose tolerance and type 2 diabetes and correlates with muscle and hepatic insulin resistance. *Diabetes Care*. 2009;32:1542–1546.
15 Lee Y, Lim S, Hong E-S, et al. Serum FGF21 concentration is associated with hypertriglyceridaemia, hyperinsulinaemia and pericardial fat accumulation, independently of obesity, but not with current coronary artery status. *Clin Endocrinol*. 2014;80:57–64.
16 Lips MA, de Groot GH, Berends FJ, et al. Calorie restriction and Roux-en-Y gastric bypass have opposing effects on circulating FGF21 in morbidly obese subjects. *Clin Endocrinol*. 2014;81:862–870.
17 Crujeiras AB, Gomez-Arbelaez D, Zulet MA, et al. Plasma FGF21 levels in obese patients undergoing energy-restricted diets or bariatric surgery: a marker of metabolic stress? *Int J Obes*. 2017;41:1570–1578.
18 Hosseinzadeh A, Roever L, Alizadeh S. Surgery-induced weight loss and changes in hormonally active fibroblast growth factors: a systematic review and meta-analysis. *Obes Surg*. 2020;30:4046–4060.
19 Gómez-Ambrosi J, Gallego-Escuredo JM, Catalán V, et al. FGF19 and FGF21 serum concentrations in human obesity and type 2 diabetes behave differently after diet- or surgically-induced weight loss. *Clin Nutr*. 2017;36:861–868.
20 American Diabetes Association. 2. Classification and diagnosis of diabetes: standards of medical care in diabetes-2019. *Diabetes Care*. 2019;42:S13–S28.
21 Verger EO, Armstrong P, Nielsen T, et al. Dietary assessment in the MetaCardis study: development and relative validity of an online food frequency questionnaire. *J Acad Nutr Diet*. 2017;117:878–888.
22 Matthews DR, Hosker JP, Rudenski AS, Naylor BA, Treacher DF, Turner RC. Homeostasis model assessment: insulin resistance and beta-cell function from fasting plasma glucose and insulin concentrations in man. *Diabetologia*. 1985;28:412–419.
23 Corcelles R, Boules M, Froylich D, et al. Total weight loss as the outcome measure of choice after Roux-en-Y gastric bypass. *Obes Surg*. 2016;26:1794–1798.
24 Krieg L, Didt K, Karkossa I, et al. Multiomics reveal unique signatures of human epiploic adipose tissue related to systemic insulin resistance. *Gut*. 2022;71(11):2179–2193.
25 Forslund SK, Chakaroun R, Zimmermann-Kogadeeva M, et al. Combinatorial, additive and dose-dependent drug-microbiome associations. *Nature*. 2021;600:500–505.
26 Bel Lassen P, Charlotte F, Liu Y, et al. The FAT score, a fibrosis score of adipose tissue: predicting weight-loss outcome after gastric bypass. *J Clin Endocrinol Metab*. 2017;102:2443–2453.
27 Huang DW, Sherman BT, Lempicki RA. Systematic and integrative analysis of large gene lists using DAVID bioinformatics resources. *Nat Protoc*. 2009;4:44–57.
28 Kursa MB, Rudnicki WR. Feature selection with theBorutaPackage. *J Stat Softw*. 2010;36. https://doi.org/10.18637/jss.v036.i11.
29 Robin X, Turck N, Hainard A, et al. pROC: an open-source package for R and S+ to analyze and compare ROC curves. *BMC Bioinf*. 2011;12. https://doi.org/10.1186/1471-2105-12-77.
30 Tingley D, Yamamoto T, Hirose K, Keele L, Imai K. Mediation: *R*package for causal mediation analysis. *J Stat Softw*. 2014;59. https://doi.org/10.18637/jss.v059.i05.
31 Machinal F. In vivo and in vitro ob gene expression and Leptin secretion in rat adipocytes: evidence for a regional specific regulation by sex steroid hormones. *Endocrinology*. 1999;140:1567–1574.
32 Zhang S, Gao J, Liu S, et al. Transcription coactivator BCL3 acts as a potential regulator of lipid metabolism through the effects on inflammation. *J Inflamm Res*. 2021;14:4915–4926.
33 Lee S, Lim G-E, Kim Y-N, Koo H-S, Shim J. AP2M1 supports TGF-β signals to promote collagen expression by inhibiting caveolin expression. *Int J Mol Sci*. 2021;22:1639.
34 Cheng R, Xu H, Hong Y. miR 221 regulates TGF-β1-induced HSC activation through inhibiting autophagy by directly targeting LAMP2. *Mol Med Rep*. 2021;24. https://doi.org/10.3892/mmr.2021.12417.
35 Osorio-Conles Ó, Vidal J, de Hollanda A. Impact of bariatric surgery on adipose tissue biology. *J Clin Med*. 2021;10:5516.
36 Zhang X, Yeung DCY, Karpisek M, et al. Serum FGF21 levels are increased in obesity and are independently associated with the metabolic syndrome in humans. *Diabetes*. 2008;57:1246–1253.
37 Qi Y, Kapterian TS, Du X, et al. CDP-diacylglycerol synthases regulate the growth of lipid droplets and adipocyte development. *J Lipid Res*. 2016;57:767–780.
38 Hong ES, Lim C, Choi HY, et al. Plasma fibroblast growth factor 21 levels increase with ectopic fat accumulation and its receptor levels are decreased in the visceral fat of patients with type 2 diabetes. *BMJ Open Diabetes Res Care*. 2019;7:e000776.
39 DeBari MK, Abbott RD. Adipose tissue fibrosis: mechanisms, models, and importance. *Int J Mol Sci*. 2020;21:6030.
40 Manca C, Pintus S, Murru E, et al. Fatty acid metabolism and derived-mediators distinctive of PPAR-α activation in obese subjects Post bariatric surgery. *Nutrients*. 2021;13:4340.
41 Lundåsen T, Hunt MC, Nilsson L-M, et al. PPARalpha is a key regulator of hepatic FGF21. *Biochem Biophys Res Commun*. 2007;360:437–440.
42 Tan BK, Hallschmid M, Adya R, Kern W, Lehnert H, Randeva HS. Fibroblast growth factor 21 (FGF21) in human cerebrospinal fluid: relationship with plasma FGF21 and body adiposity. *Diabetes*. 2011;60:2758–2762.
43 Vinales KL, Begaye B, Bogardus C, Walter M, Krakoff J, Piaggi P. FGF21 is a hormonal mediator of the human "thrifty" metabolic phenotype. *Diabetes*. 2019;68:318–323.
44 Jensen-Cody SO, Flippo KH, Claflin KE, et al. FGF21 signals to glutamatergic neurons in the ventromedial hypothalamus to suppress carbohydrate intake. *Cell Metab*. 2020;32:273–286.e6.
45 Claflin KE, Sullivan AI, Naber MC, et al. Pharmacological FGF21 signals to glutamatergic neurons to enhance leptin action and lower body weight during obesity. *Mol Metab*. 2022;64:101564.
46 Jansen PLM, van Werven J, Aarts E, et al. Alterations of hormonally active fibroblast growth factors after Roux-en-Y gastric bypass surgery. *Dig Dis*. 2011;29:48–51.
47 Gómez-Ambrosi J, Silva C, Galofré JC, et al. Body mass index classification misses subjects with increased cardiometabolic risk factors related to elevated adiposity. *Int J Obes*. 2012;36:286–294.
48 Pérez-Martí A, Garcia-Guasch M, Tresserra-Rimbau A, et al. A low-protein diet induces body weight loss and browning of subcutaneous white adipose tissue through enhanced expression of hepatic fibroblast growth factor 21 (FGF21). *Mol Nutr Food Res*. 2017;61:1600725.
49 Frayling TM, Beaumont RN, Jones SE, et al. A common allele in FGF21 associated with sugar intake is associated with body shape, lower total body-fat percentage, and higher blood pressure. *Cell Rep*. 2018;23:327–336.
50 Dushay J, Chui PC, Gopalakrishnan GS, et al. Increased fibroblast growth factor 21 in obesity and nonalcoholic fatty liver disease. *Gastroenterology*. 2010;139:456–463.
51 Berti L, Irmler M, Zdichavsky M, et al. Fibroblast growth factor 21 is elevated in metabolically unhealthy obesity and affects lipid deposition, adipogenesis, and adipokine secretion of human abdominal subcutaneous adipocytes. *Mol Metab*. 2015;4:519–527.
52 Chen Z, Yang L, Liu Y, Huang P, Song H, Zheng P. The potential function and clinical application of FGF21 in metabolic diseases. *Front Pharmacol*. 2022;13:1089214.
53 Debédat J, Sokolovska N, Coupaye M, et al. Long-term relapse of type 2 diabetes after roux-en-Y gastric bypass: prediction and clinical relevance. *Diabetes Care*. 2018;41:2086–2095.
54 De Luca A, Delaye J-B, Fauchier G, et al. 3-month post-operative increase in FGF21 is predictive of one-year weight loss after bariatric surgery. *Obes Surg*. 2023;33:2468–2474.
55 Kersten S. Integrated physiology and systems biology of PPARα. *Mol Metab*. 2014;3:354–371.
56 Morrison CD, Hao Z, Mumphrey MB, et al. Roux-en-Y gastric bypass surgery is effective in fibroblast growth factor-21 deficient mice. *Mol Metab*. 2016;5:1006–1014.
57 Gerhard GS, Styer AM, Strodel WE, et al. Gene expression profiling in subcutaneous, visceral and epigastric adipose tissues of patients with extreme obesity. *Int J Obes*. 2014;38:371–378.